Origin of Paleoproterozoic Komatiites at Jeesiörova, Kittilä Greenstone Complex, Finnish Lapland

AMITAVA GANGOPADHYAY[1]*, RICHARD J. WALKER[1], EERO HANSKI[2] AND PETER A. SOLHEID[3]

[1]ISOTOPE GEOCHEMISTRY LABORATORY, DEPARTMENT OF GEOLOGY, UNIVERSITY OF MARYLAND, COLLEGE PARK, MD 20742, USA

[2]DEPARTMENT OF GEOSCIENCES, UNIVERSITY OF OULU, P.O. BOX 3000, FIN-90014 UNIVERSITY OF OULU, FINLAND

[3]INSTITUTE FOR ROCK MAGNETISM, 291 SHEPHERD LABS, 100 UNION STREET S.E., MINNEAPOLIS, MN 55455-0128, USA

Komatiites from the ~2 Ga Jeesiörova area in Finnish Lapland have subchondritic Al_2O_3/TiO_2 ratios like those in Al-depleted komatiites from Barberton, South Africa. They are distinct in that their Al abundances are higher than those of the Al-depleted rocks and similar to levels in Al-undepleted komatiites. Moderately incompatible elements such as Ti, Zr, Eu, and Gd are enriched. Neither majorite fractionation nor hydrous melting in a supra-subduction zone setting could have produced these komatiites. Their high concentrations of moderately incompatible elements may have resulted from contamination of their parental melt through interaction with metasomatic assemblages in the lithospheric mantle or enrichment of their mantle source in basaltic melt components. Re–Os isotope data for chromite from the Jeesiörova rocks yield an average initial $^{187}Os/^{188}Os$ of 0·1131 ± 0·0006 (2σ), $\gamma_{Os}(I) = 0·1 \pm 0·5$. These data, coupled with an initial ε_{Nd} of ~+4, indicate that melt parental to the komatiites interacted minimally with ancient lithospheric mantle. If their mantle source was enriched in a basaltic component, the combined Os–Nd isotopic data limit the enrichment process to within ~200 Myr prior to the formation of the komatiites. Their Os–Nd isotopic composition is consistent with derivation from the contemporaneous convecting upper mantle.

KEY WORDS: *Finnish Lapland; Jeesiörova; komatiites; mantle geochemistry; petrogenesis; redox state; Re/Os isotopes; Ti enrichment*

INTRODUCTION

Komatiites have been divided into two broad chemical types, Al-undepleted (with near-chondritic Al_2O_3/TiO_2 ratios of ~22) and Al-depleted (subchondritic Al_2O_3/TiO_2 ratios of typically ~11), e.g. Nesbitt *et al.* (1979). Komatiites from Alexo and Pyke Hill in the Abitibi greenstone belt, Canada, are typical examples of the Al-undepleted type (also termed 'Munro-type'; Pyke *et al.*, 1973; Arndt, 1986), whereas those from the Komati and Mendon Formations in the Barberton Mountainland, South Africa, are examples of the Al-depleted type (also known as the 'Barberton-type'; Nesbitt & Sun, 1976). The komatiitic rocks from the Jeesiörova area in the Central Lapland Greenstone Belt, northern Finland (Fig. 1) are distinct from these two types of komatiite in that they have subchondritic Al_2O_3/TiO_2 ratios (typically ~10–13), similar to those in Al-depleted rocks, yet compared with the latter they have significantly higher aluminum contents at given MgO levels (Hanski *et al.*, 2001; Fig. 2a). However, the aluminum contents in the Jeesiörova rocks are similar to those of Al-undepleted komatiites at given MgO contents. In addition, the Jeesiörova rocks have significantly higher TiO_2 contents at given MgO and Al_2O_3 contents than either Al-depleted or Al-undepleted komatiites from elsewhere (Fig. 2b). This distinctive combination of bulk-rock

*Corresponding author. Present address: Geochemistry Division, National High Magnetic Field Laboratory, 1800 E. Paul Dirac Drive, Tallahassee, FL 32310, USA. Telephone: +1-850-645-2486. Fax: +1-850-644-0827. E-mail: amitava@magnet.fsu.edu
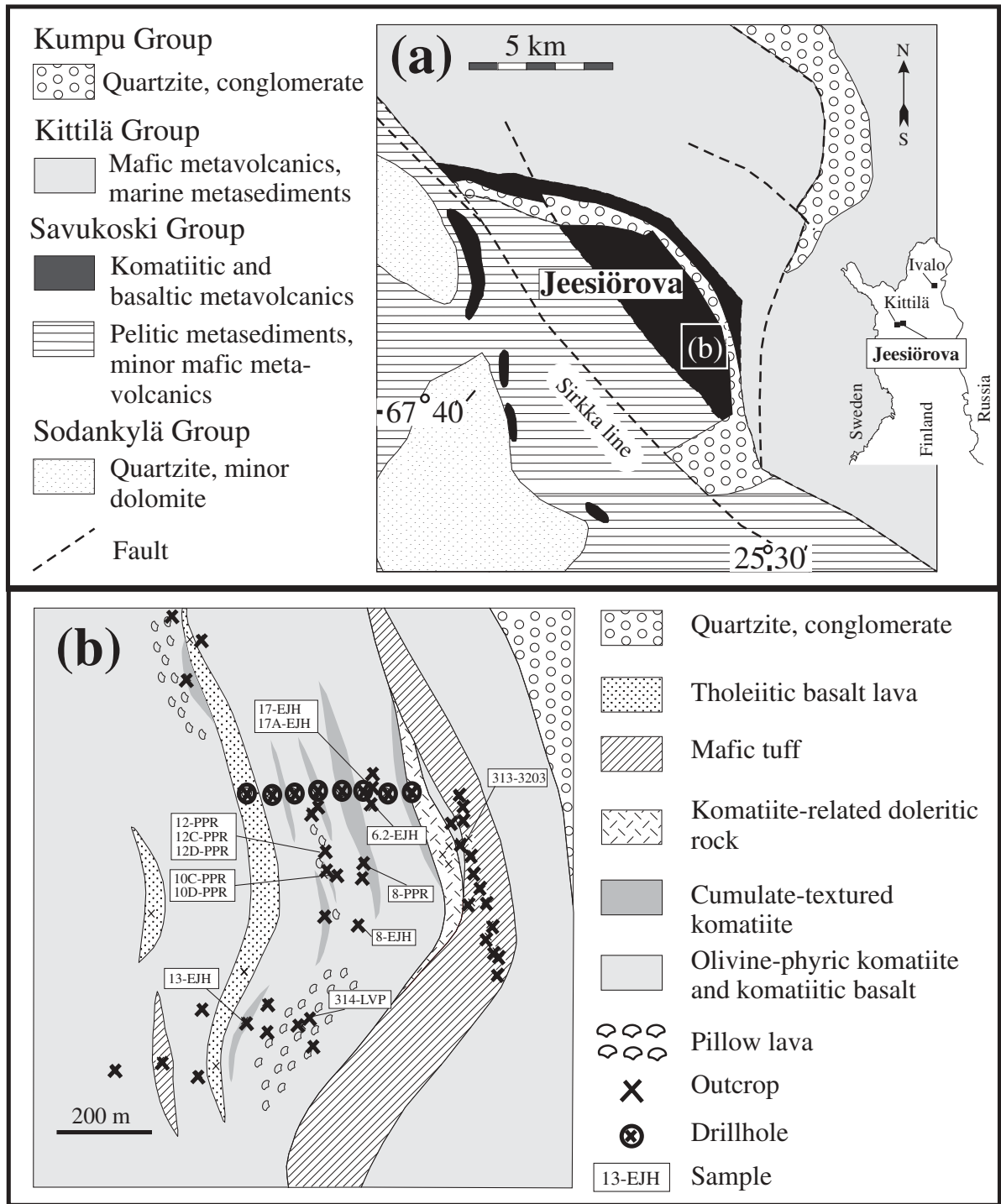
Fig. 1. (a) Geological map of the Jeesiörova area, central Finnish Lapland. (b) Detailed map of the Jeesiörova area showing sample locations.

chemical characteristics for the Jeesiörova rocks prompted construction of a new classification scheme for komatiites using olivine-projected molecular Al_2O_3–TiO_2 relations (Hanski *et al.*, 2001). The Jeesiörova rocks, according to this scheme, plot in a distinct field of 'Ti-enriched' komatiites. Aluminum-depleted, Al-undepleted and/or Ti-enriched rock types can coexist in a single greenstone belt and, in some cases, within a single volcanic assemblage (e.g. Kidd–Munro assemblage in the Abitibi greenstone belt, Canada: Sproule *et al.*,
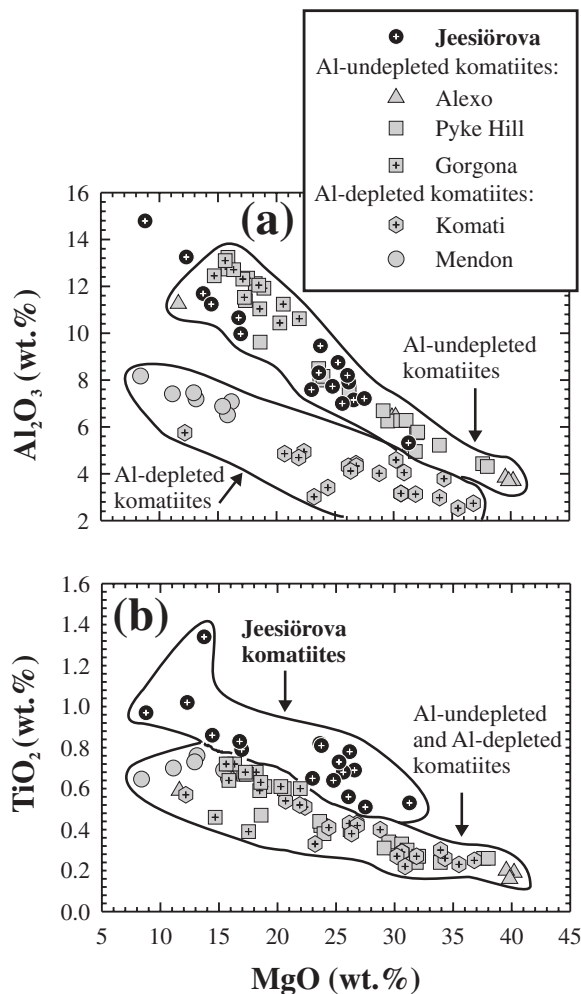
Fig. 2. (a) Whole-rock MgO vs Al_2O_3 (wt %) in the Jeesiörova komatiitic rocks. Also plotted for comparison are Al-undepleted komatiites (Alexo and Pyke Hill in the Abitibi greenstone Belt, Canada, and Gorgona, Colombia) and Al-depleted komatiites (Komati and Mendon Formations in the Barberton Mountainland, South Africa). Data sources: Alexo, Gangopadhyay & Walker (2003); Pyke Hill, Fan & Kerrich [(1997), combined with new unpublished data: n = 7]; Gorgona, Echeverria (1980) and Arndt *et al.* (1997); Komati, Lahaye *et al.* (1995) and Parman *et al.* (2003); Mendon, Lahaye *et al.* (1995). All data are volatile-free values. (b) MgO vs TiO_2 (wt %) in the same suites of rocks as in (a).

2002). It is important to determine, therefore, whether the apparent Ti enrichment is a feature of the mantle source, and if so, what the implications of Ti enrichment are for the nature of the source and the petrogenetic processes involved in komatiite magma genesis.

Here we compare and contrast the petrological, geochemical and isotopic characteristics of the Jeesiörova komatiites with those of the well-studied Munro and Barberton type komatiites in order to assess the origin of the Finnish rocks. We present electron microprobe data for chromites from the Finnish suite of rocks, and use them in conjunction with the $Fe^{3+}/\Sigma Fe$ ratios of selected

chromite separates determined by Mössbauer spectroscopy in order to constrain the redox state of the parental magmas. Additionally, we present high-precision Re–Os isotope data for chromites in order to determine the initial Os isotopic composition of the mantle source of this chemically distinct type of komatiite. The initial Os isotopic composition, combined with previous estimates of the initial Nd isotopic composition of the same suite of rocks (Hanski *et al.*, 2001), is used to evaluate the possible roles of (1) contamination by crustal materials or hypothesized metasomatized lithospheric mantle mineral assemblages rich in Ti and other moderately incompatible elements, and (2) recycling of oceanic crust in the generation of these rocks. Finally, we use previously published major and trace element data for the same suite of rocks (Hanski *et al.*, 2001) to evaluate possible petrogenetic models.

GEOLOGICAL SETTING AND ROCK TYPES

Samples were collected from the Jeesiörova area, located in the southern part of the Kittilä Greenstone Complex, Central Lapland (Fig. 1a). Detailed discussions of the stratigraphic subdivisions, major rock types of the Kittilä Greenstone Complex, and their petrological and geochemical characteristics have been given by Lehtonen *et al.* (1998) and Hanski *et al.* (2001). In brief, the Kittilä Greenstone Complex is part of an ∼400 km long belt, which runs through Finnish Lapland and extends to the Karasjok greenstone belt in northern Norway (Barnes & Often, 1990). The entire belt contains abundant, highly magnesian volcanic rocks that vary in chemical composition from light rare earth element (LREE)-depleted komatiites to LREE-enriched picrites (Hanski *et al.*, 2001). A characteristic feature of the belt is the presence of ultramafic volcaniclastic rocks that vary from agglomerate-like deposits to fine-grained, laminated tuffs (Saverikko, 1985; Barnes & Often, 1990). Komatiitic rocks also occur as massive lavas, pillow lavas, and associated pillow breccias.

The Jeesiörova komatiites occur in a zone that is ∼15 km long and 4 km wide (Fig. 1a). They form part of the Savukoski Group together with underlying pelitic metasedimentary rocks. A fault zone, called the 'Sirkka line', separates the Savukoski Group rocks from younger (∼2·0 Ga) basaltic metavolcanic rocks and metasedimentary rocks of the Kittilä Group that crop out on the NE side of the Jeesiörova area. The clastic metasedimentary rocks of the Sodankylä Group are the oldest (2·3 Ga) rocks in the area, whereas the youngest supracrustal rocks are represented by the quartzites and conglomerates of the ∼1·88 Ga Kumpu Group, which lie unconformably on the rocks of the Savukoski and Kittilä Groups.

Drill cores through the lower contact of the komatiite-bearing lava succession in the Jeesiörova area show that the volcanic sequence was deposited on a 20 m thick unit of cherts and carbonate rocks that are underlain by black schists. The volcanism started with 20 m of tholeiitic lavas, followed by volcaniclastic komatiites (50 m) and finally by massive komatiitic lavas (>100 m). The total thickness of the volcanic rocks is difficult to estimate but may reach several hundreds of meters.

The bedrock in this part of the Jeesiörova area (Fig. 1b) is dominated by olivine-phyric komatiitic rocks. As a result of limited outcrops, individual lava flows cannot be delineated. There are, however, zones of cumulate-textured komatiites that probably represent the lower parts of thick lava flows. Komatiitic rocks also occur as pillow lavas with the pillow size varying from 0·2 to 1 m. Various mafic rocks are interbedded with the ultramafic rocks (Fig. 1b). The mafic rocks include LREE-depleted tuffs and dolerites. There are also mafic amygdaloidal lava flows, marked as tholeiites in Fig. 1b, which are moderately LREE enriched and probably not genetically related to the associated komatiites.

SAMPLES

The samples that form the basis of this study are all komatiites collected from outcrops (sample locations are shown in Fig. 1b), and are well characterized in terms of their major and trace element, and Sm–Nd isotope compositions (Hanski et al., 2001).

Whole-rock samples were first crushed into millimeter-sized pieces. The freshest unaltered pieces were ground in a steel pan. Different aliquots of the same whole-rock powder were used for major and trace element and isotopic analysis of each sample.

Mineral separates (chromite, clinopyroxene, and sulfide) were obtained using standard crushing, milling, concentration table, and heavy liquid techniques. Separation of large quantities of chromite was possible because of their relatively large grain size and well-preserved nature (low magnetic susceptibility). After removing the most magnetic fraction with a hand magnet, the chromite separates were divided into different fractions, depending on the degree of alteration (presence of magnetite rim) and using different current settings in a Frantz™ magnetic separator. Likewise, for sulfide separates, we obtained a fraction dominated by pentlandite, whereas the other fractions were mixtures containing pyrrhotite, pentlandite, and chalcopyrite.

ANALYTICAL TECHNIQUES

Details of the whole-rock chemical compositions of the komatiites have been reported elsewhere (Hanski et al.,

2001). Whole-rock X-ray fluorescence (XRF) data for major and minor elements were obtained using a Phillip PW 1480 spectrometer at the Geological Survey of Finland (GSF) and a Phillips PW 1410 spectrometer at the University of Tasmania (UT). The concentrations of REE and other trace elements were determined by inductively coupled plasma mass spectrometry (ICP-MS) using a Perkin-Elmer Sciex Elan 5000 instrument at the GSF and an HP 4500 instrument at the UT. The whole-rock major and trace element data of Hanski et al. (2001) are supplemented by two additional samples (10C-PPR and 314-LVP). The complete dataset is included in Electronic Appendix 1 (http://www.petrology.oxfordjournals.org).

Electron microprobe

The chemical compositions of chromites from selected samples were determined using a Cameca Camebax SX50 microprobe at the GSF (Table 1). The analytical conditions included an accelerating potential of 25 kV, a sample current of 47 nA, and a beam diameter of 1 μm.

Mössbauer analyses

Mössbauer spectra were collected for five selected chromite separates at the Institute for Rock Magnetism at the University of Minesota, Minneapolis. The chromite separates were crushed and ~20–30 mg of powder was dispersed in powdered sugar in a 12 mm diameter sample holder. The spectra were collected at room temperature using a constant acceleration transmission spectrometer with a ^{57}Co in Rh matrix source and an activity of ~5 mC. The spectra were fitted with four doublets and two sextets using a least-squares fitting routine. The hyperfine parameters as well as peak area and width were allowed to float with no bounds enforced. Three of the samples, 12-PPR, 10C-PPR and 6.2-EJH, have significant amounts of a magnetically ordered phase with the hyperfine parameters consistent with magnetite. Of the four doublets that were fitted for all of the samples, three can be assigned to Fe^{2+} with isomer shifts above 0·63 mm/s and quadrupole splitting above 1·2 mm/s, and one can be assigned to Fe^{3+} with isomer shift ranging from 0·16 to 0·45 mm/s and quadrupole splitting between 0·53 and 0·86 mm/s. Although some ambiguity exists because of the three overlapping Fe^{2+} doublets, the overall area assignment to Fe^{2+} is not affected excepting only the relation between the Fe^{2+} doublets. The Fe^{2+}/Fe^{3+} ratios were calculated from the paramagnetic doublets as defined above. In order to calculate the $Fe^{3+}/\Sigma Fe$ ratios of paramagnetic iron, we excluded the iron in the magnetite. Assuming stoichiometry, magnetite can be expressed as $Fe^{3+}[Fe^{2+}Fe^{3+}]O_4$ with the tetrahedral site containing only Fe^{3+} and the octahedral site containing equal contents of Fe^{2+} and Fe^{3+}. The

Table 1: Representative electron microprobe analyses of chromites from the Jeesiörova komatiites

Sample:	13-EJH	6.2-EJH	12C-PPR	17-EJH	10C-PPR	12D-PPR	8-PPR	10D-PPR	12-PPR
SiO_2	0·11	0·14	0·06	0·07	0·05	0·05	0·06	0·08	0·10
TiO_2	0·40	0·44	0·58	0·47	0·60	0·69	0·75	0·51	0·55
Al_2O_3	13·98	13·16	14·54	13·55	13·45	14·93	16·04	13·39	13·82
Cr_2O_3	47·43	51·13	50·90	49·67	50·96	48·92	44·92	54·23	52·33
V_2O_3	n.d.	n.d.	n.d.	n.d.	n.d.	n.d.	0·24	0·11	0·17
Fe_2O_3*	8·53	5·58	6·01	7·03	6·38	6·75	9·23	4·70	5·43
FeO	16·06	15·93	11·57	15·86	13·31	12·12	14·78	10·19	11·18
MnO	0·14	0·12	0·07	0·12	0·00	0·06	0·25	0·09	0·21
MgO	11·64	11·78	14·91	11·89	13·66	14·50	13·00	15·73	15·05
CaO	0·10	0·02	0·00	0·03	0·01	0·01	0·02	0·00	0·01
CoO	0·03	0·03	0·03	0·03	0·03	0·02	0·00	0·02	0·00
NiO	0·16	0·15	0·22	0·18	0·19	0·22	0·23	0·23	0·23
ZnO	n.d.	n.d.	n.d.	n.d.	n.d.	n.d.	0·07	0·03	0·03
Total	98·57	98·48	98·90	98·89	98·64	98·26	99·59	99·31	99·11
Cr-no.	0·695	0·723	0·701	0·711	0·718	0·687	0·653	0·731	0·717
Mg-no.	0·564	0·569	0·697	0·572	0·647	0·681	0·611	0·733	0·706
Fe^{3+}-no.	0·106	0·070	0·073	0·087	0·079	0·083	0·113	0·057	0·066
$Fe^{3+}/\Sigma Fe$		0·27			0·21		0·28	0·16	0·22

*Fe_2O_3 and FeO were distributed based on calculations assuming stoichiometry.
All analyses were obtained from the cores of equant grains. n.d., not determined. Cr-number = Cr/(Cr + Al), Mg-number = Mg/(Mg + Fe^{2+}) and Fe^{3+}-number = Fe^{3+}/(Fe^{3+} + Cr + Al) (all in atomic proportions). $Fe^{3+}/\Sigma Fe$ was determined by Mössbauer spectroscopy.

ferric/ferrous ratios of selected chromite separates obtained through analyses of Mössbauer spectra are included in Table 1.

Re–Os isotope analyses

The chemical separation techniques for Re–Os analysis employed in this study follow previously published work (Shirey & Walker, 1995; Cohen & Waters, 1996) and have been described in detail elsewhere (Gangopadhyay & Walker, 2003; Gangopadhyay, 2004; Gangopadhyay *et al.*, 2005). Approximately 3 g of whole-rock powder was dissolved in reverse aqua regia, and frozen and equilibrated with spikes in sealed Pyrex™ Carius tubes. The tubes containing whole-rock powder were heated at 240°C for at least 24 h, whereas those with mineral separates (chromite, clinopyroxene and sulfide) were heated for at least 48 h to facilitate complete digestion. Osmium was separated by solvent extraction into carbon tetrachloride and finally transferred into concentrated HBr (Cohen & Waters, 1996). The final purification for Os was accomplished via micro-distillation. Rhenium was recovered from aqua regia via anion exchange column chemistry (Morgan & Walker, 1989).

The isotopic compositions of Re and Os were obtained using negative thermal ionization mass spectrometry (Creaser *et al.*, 1991; Völkening *et al.*, 1991). The mass spectrometric procedures followed in this study have been discussed by Walker *et al.* (1994) and Morgan *et al.* (1995). Samples with high Os abundances (whole-rock, chromite and sulfide) were analyzed with Faraday cups in the static mode (using a Sector 54 mass spectrometer), whereas those with relatively low abundances of Os (e.g. clinopyroxene) and/or Re (e.g. chromite) were analyzed with an electron multiplier using a 12″ NBS mass spectrometer.

The total ranges in analytical blanks for Re and Os were 1·2–6·4 pg (excluding one outlier with 12·7 pg of Re) and 1·3–6·9 pg (*n* = 6), respectively, and are negligible compared with their concentrations in most of the whole-rock samples. The blank contribution, however, was substantial (typically between 2 and 10%) for some of the Re analyses of chromites. The isotopic compositions of the blanks were natural for Re and $^{187}Os/^{188}Os$ varied between 0·135 and 0·223 (excepting one outlier with 0·319). All data were corrected for blanks and the isotopic and concentration data in Table 2 represent the corrected values. The uncertainties in blanks are reflected in respective uncertainties for isotopic and concentration data in Table 2. The external reproducibilities on standard analyses for Os and Re are typically better than ±0·1 and ±0·3%, respectively.

Table 2: Re and Os concentrations and isotope compositions for the whole-rock Jeesiörova komatiites and mineral separates

Sample	Re (ppb)	Os (ppb)	^{187}Re/^{188}Os	^{187}Os/^{188}Os	$\gamma_{Os}(T)$*	Model ages (Ga)
Whole-rocks						
8-PPR	0·5715	2·734	1·011	0·15978	+10 ± 0·3	
10D-PPR	0·7815	4·788	0·7885	0·14789	+6·6 ± 0·5	
12-PPR	0·5438	6·166	0·4254	0·13638	+7·6 ± 0·2	
12C-PPR	0·8238	5·758	0·6905	0·14001	+2·6 ± 0·2	
6.2-EJH	0·9671	3·013	1·554	0·16351	−3·2 ± 0·3	
8-EJH	0·3341	1·284	1·266	0·20185	+40 ± 0·5	
12D-PPR	0·6362	5·135	0·5976	0·13628	+2·2 ± 0·2	
17-EJH	0·4132	2·345	0·8527	0·16111	+16 ± 0·3	
17A-EJH	0·8862	2·696	1·591	0·16322	−4·6 ± 0·3	
313-3203	0·0590	1·389	0·2048	0·13190	+10 ± 0·4	
10C-PPR	0·5008	3·860	0·6256	0·13322	−1·4 ± 0·2	
Chromites						
10C-PPR	0·732	102·1	0·0345	0·11404	−0·2 ± 0·2	
Dupl.	0·790	121·0	0·0314	0·11397	−0·1 ± 0·1	
Trpl.	1·18	77·41	0·0736	0·11520	−0·3 ± 0·1	
314-LVP	0·711	75·91	0·0451	0·11569	+1·0 ± 0·4	
Dupl.	0·946	65·99	0·0689	0·11645	+0·9 ± 0·5	
8-PPR	0·433	84·53	0·0246	0·11371	−0·1 ± 0·1	
8-PPR/2	0·437	70·84	0·0296	0·11404	0·0 ± 0·4	
12C-PPR	0·471	161·9	0·0140	0·11342	−0·1 ± 0·1	
12D-PPR/2	0·722	223·2	0·0156	0·11342	−0·1 ± 0·2	
10D-PPR	0·887	53·80	0·0793	0·11556	−0·2 ± 0·6	
17A-EJH	0·901	84·46	0·0513	0·11368	−1·0 ± 0·6	
Clinopyroxenes						
10D-PPR	1·388	1·118	6·209	0·42027	+80	
12-PPR†	2·178	153·4	0·0683	0·11812	+2·4	
12D-PPR	0·2226	0·7118	1·520	0·19442	+25	
17-EJH	0·6252	6·895	0·4374	0·13525	+6·2	
17A-EJH	0·3711	0·9037	2·000	0·21212	+26	
Dupl.	0·2935	0·4224	3·427	0·31007	+69	
12C-PPR	0·9818	0·5503	9·007	0·49843	+63	
Dupl.	0·8444	0·5233	8·134	0·48341	+77	
Sulfides						
10C-PPR	59·56	2·942	156·5	4·8617	−624	1·8
Dupl.	59·73	4·730	80·47	2·6248	−258	1·8
10D-PPR	167·5	5·042	410·2	13·067	−1186	1·9
Dupl.	195·8	5·410	503·1	14·917	−2410	1·7
12C-PPR‡	270·1	6·176	2008	67·751	−2070	2·0

Total analytical uncertainties are 0·3% for ^{187}Re/^{188}Os and 0·1% for ^{187}Os/^{188}Os (2σ). For clinopyroxenes, the uncertainties on ^{187}Os/^{188}Os ratios are ±0·3% (2σ). All Os analyses, except for clinopyroxenes, were performed on a Faraday cup, whereas all Re analyses (except for sulfides) were made using an electron multiplier. Dupl. and Trpl. denote duplicate and triplicate analyses of different aliquots of powder, respectively.
*Calculated values at the Sm−Nd regression age of 2·056 Ga (Hanski *et al.*, 2001). The projected chondritic ^{187}Os/^{188}Os at 2·056 Ga is calculated to be 0·11300, using the average ^{187}Re/^{188}Os ratio of chondrites and initial ^{187}Os/^{188}Os (at T = 4·558 Ga) for early Solar System materials (IIIA irons) of 0·40186 and 0·09531, respectively (Shirey & Walker, 1998), and λ (^{187}Re → ^{187}Os + β$^-$) = 1·666 × 10^{-11} year^{-1} (Smoliar *et al.*, 1996).
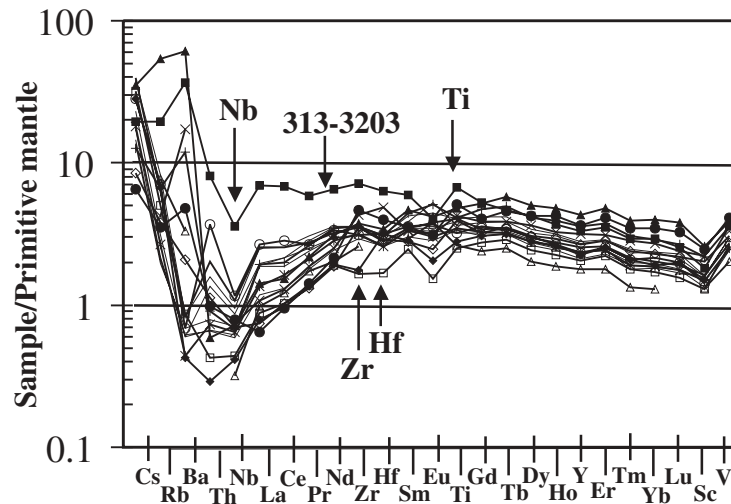†Clinopyroxene + chromite.
‡Pentlandite.

Fig. 3. Primitive mantle (PM)-normalized (McDonough & Sun, 1995) extended REE diagram for the whole-rock Jeesioröva komatiites. The only sample (313-3203) that shows LREE enrichment is labeled.

RESULTS

Whole-rock geochemical characteristics

The Jeesiörova komatiites have subchondritic Al_2O_3/TiO_2 ratios and characteristic chondrite-noma-lized (CN) heavy rare earth element (HREE)-depleted patterns ($Gd/Yb_{CN} >1$), similar to those typical of Al-depleted komatiites (e.g. Lahaye *et al.*, 1995). Additionally, the Jeesiörova rocks have high abundances of high field strength elements (HFSE; e.g. Ti, Zr) and moderately incompatible REE (e.g. Nd, Sm, Eu, Gd) relative to those at a given MgO content in both Al-depleted and Al-undepleted komatiites (Fig. 2b; also see Hanski *et al.*, 2001). In contrast to high concentrations of Ti and Zr, virtually all Jeesiörova samples show negative Nb anomalies and characteristic depletions in LREE (Fig. 3).

Re–Os concentrations and isotopic compositions

Re–Os concentrations and isotopic compositions for the whole-rocks and mineral separates (chromite, clinopyroxene and sulfide) are reported in Table 2. The concentrations of Re and Os, and Re/Os ratios for all the sample types are plotted in Fig. 4a and b. The abundances of both Os and Re vary over two orders of magnitude (Fig. 4a). The Os concentrations are highest in chromite and lowest in clinopyroxene separates.

The very high concentrations of Os, coupled with low Re concentrations in chromite, result in very low Re/Os ratios (Fig. 4b). The Re–Os isotope data for the chromites do not yield a precise isochron as a result of the very limited spread in their $^{187}Re/^{188}Os$ ratios (∼0·01–0·07: Table 2) and relatively large uncertainties in Re concentrations. Because of their low Re/Os ratios and minimal
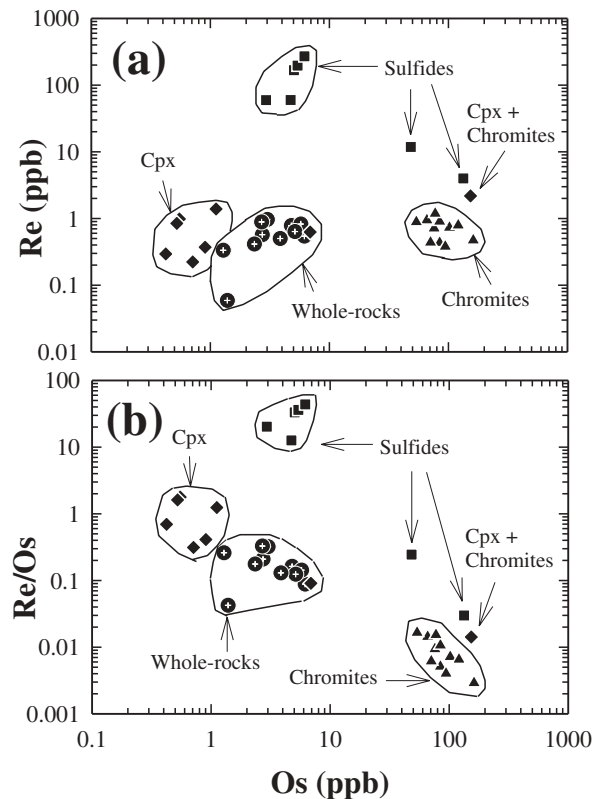

Fig. 4. Plot of (a) concentrations of Re and Os (ppb) in whole-rocks and mineral separates (clinopyroxene, sulfide, and chromite) from the Jeesiörova komatiites. (b) Os concentrations of the same samples as in (a) plotted against Re/Os.

correction of $^{187}Os/^{188}Os$ for age, chromites were used to precisely determine the initial $^{187}Os/^{188}Os$ for these rocks. The average initial $^{187}Os/^{188}Os$ ratio obtained for the chromites (0·1131 ± 0·0006, 2σ) corresponds to a γ_{Os}
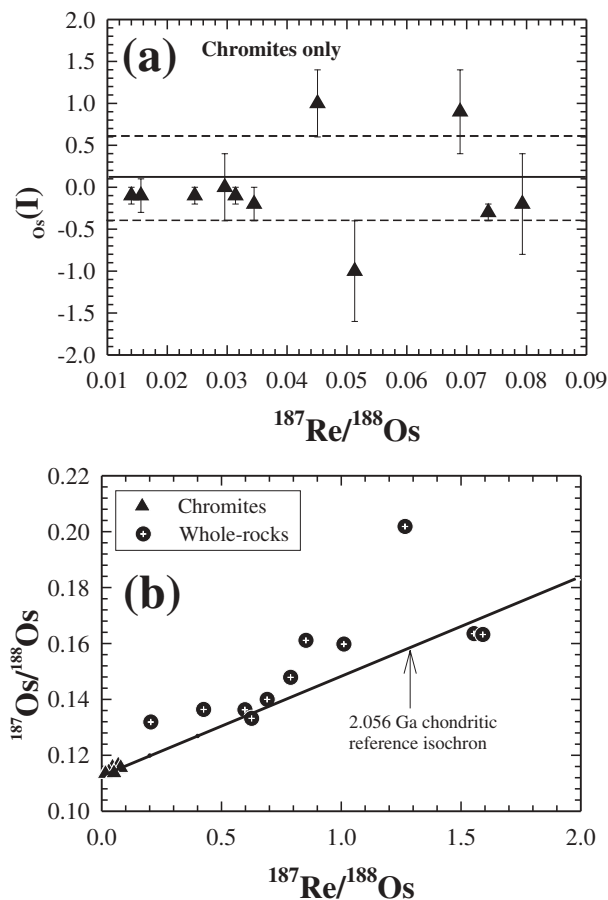
Fig. 5. (a) Initial γ_{Os}(I) (at the crystallization age of 2·056 Ga: Hanski *et al.*, 2001) vs $^{187}Re/^{188}Os$ of chromites from the Jeesiörova komatiites. The continuous horizontal line represents the calculated initial γ_{Os}(I), and the dashed lines show the upper and lower limits of γ_{Os}(I) corresponding to the 2σ variations in the calculated average initial $^{187}Os/^{188}Os$ for the chromites. (b) $^{187}Re/^{188}Os$ vs $^{187}Os/^{188}Os$ for whole-rock Jeesiörova komatiites and their chromite separates.

of 0·1 ± 0·5 at the 2·056 Ga age of crystallization (Fig. 5a). This precisely chondritic average initial Os isotopic composition is indistinguishable from the projected Os isotopic composition of the contemporaneous convecting upper mantle (Snow & Reisberg, 1995; Walker *et al.*, 1996, 2002; Brandon *et al.*, 2000).

The concentrations of Os in the whole-rocks are typically high, varying between ~1·3 and 6·2 ppb (Fig. 4b). Similarly, the whole-rock Re concentrations are high (mostly above 0·5 ppb) relative to komatiites from elsewhere (e.g. Gangopadhyay & Walker, 2003; Gangopadhyay *et al.*, 2005). The whole-rock samples mostly plot above a chondritic reference isochron (Fig. 5b) and display a large variation in their respective calculated initial γ_{Os} values (Table 2).

The sulfide separates have the highest Re concentrations and most of them have very high Re/Os ratios

(Fig. 4b). The sulfide separates give generally consistent Os model ages of ~1·8 Ga. This model age is ~250 Myr younger than the Sm–Nd age of these rocks (2056 ± 25 Myr: Hanski *et al.*, 2001). This suggests that the primary Re–Os systematics of the sulfides were disturbed ~250 Ma after their crystallization because of secondary processes such as hydrothermal alteration and/or metamorphic resetting. As a result, the sulfides give anomalous initial γ_{Os} values for the crystallization age of the rocks (Table 2). It is not uncommon for the Re–Os system to display open-system behavior in sulfide phases associated with komatiites (e.g. Luck & Allègre, 1984; Shirey & Walker, 1995; Walker *et al.*, 1997).

Clinopyroxene separates have both relatively high Os (>0·5 ppb to ~1 ppb, excepting one separate, 17-EJH) and Re concentrations (up to ~1·4 ppb). Clinopyroxene separates have highly variable initial γ_{Os} values (ranging between +6 and +80). Most of the whole-rock and clinopyroxene separates in these rocks give generally consistent initial Nd isotopic compositions (Hanski *et al.*, 2001), whereas the Re–Os isotope systematics of these samples indicate large-scale open-system behavior. This may be due to the presence of secondary sulfide inclusions within clinopyroxene or sulfide impurities in our clinopyroxene separates.

DISCUSSION

Are the Jeesiörova komatiites Al depleted?

The low Al_2O_3/TiO_2 ratios of the Jeesiörova komatiites could result from depletion in Al or enrichment in Ti relative to the Al-undepleted Munro-type komatiites. Several aspects of the Jeesiörova rocks suggest that the parental liquids were not Al depleted. First, the bulk aluminum contents at given MgO levels of the Jeesiörova rocks are significantly higher than in the Al-depleted Barberton rocks, and similar to those in Al-undepleted Munro rocks (Fig. 2a). Second, the chromites in the Jeesiörova rocks have distinctly higher Al contents than those in the Al-depleted komatiites from elsewhere (Barnes & Roeder, 2001; Fig. 6a). The chromites in the Finnish rocks are, on the other hand, chemically similar to chromites from the Al-undepleted komatiites from Gorgona Island (Echeverria, 1980) and Pyke Hill in the Munro Township (Arndt *et al.*, 1977; Fig. 6a). The similar aluminum contents of the chromites in both the Jeesiörova rocks and those in Al-undepleted komatiites from Pyke Hill, Canada (Arndt *et al.*, 1977), Vetreny, Russia (Puchtel *et al.*, 1996) and Belingwe, Zimbabwe (Zhou & Kerrich, 1992) are also apparent in Fig. 6b. Combined, these characteristics suggest that aluminum contents in the magmas parental to the Finnish rocks were more similar to those of Al-undepleted, rather than Al-depleted rocks.
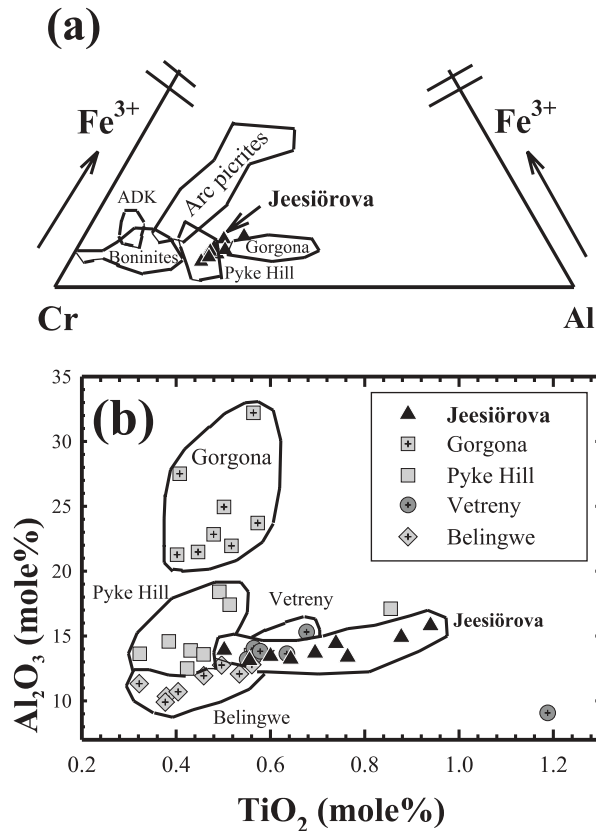
Fig. 6. (a) Trivalent cations ($Al–Cr–Fe^{3+}$) in chromites from the Jeesiörova rocks compared with Al-undepleted Pyke Hill (Arndt *et al.*, 1977) and Gorgona (Echeverria, 1980) komatiites. The approximate positions of the fields of Al-depleted komatiites (ADK) and boninites are shown after Barnes & Roeder (2001). The field for arc-related picrites is based on data from Eggins (1993). (b) Al_2O_3 vs TiO_2 (mol %) in chromites from Jeesiörova komatiites, compared with those from Al-undepleted komatiites (Gorgona, Pyke Hill, Vetreny, and Belingwe). Data sources: Gorgona, Echeverria (1980); Pyke Hill, Arndt *et al.* (1977); Vetreny, Puchtel *et al.* (1996); Belingwe, Zhou & Kerrich (1992).

As noted, the Jeesiörova komatiites have high concentrations of moderately incompatible elements, but are depleted in both more incompatible (LREE) and less incompatible elements (HREE). As a result, these rocks show characteristic convex-up patterns in mantle-normalized trace element diagrams (Fig. 3). In addition, they have subchondritic Al_2O_3/TiO_2 ratios similar to those commonly observed in Al-depleted komatiites (Nesbitt & Sun, 1976; Herzberg, 1995; Lahaye *et al.*, 1995).

Previous studies of Al-depleted Barberton-type komatiites (e.g. Lahaye *et al.*, 1995) have documented negative correlations between HREE depletions (e.g. $Gd/Yb_{CN} > 1$) and HFSE anomalies [e.g. $Zr/Zr^* = Zr/10^{(\log Sm + \log Nd)/2}$: McCuaig *et al.*, 1994]. These features have been explained by separation of the high-pressure form of garnet (majorite garnet at $>14\,GPa$) in

the deep mantle (Yurimoto & Ohtani, 1992; Xie & Kerrich, 1994; Lahaye *et al.*, 1995). This interpretation was based on the close correspondence between the variations in HFSE and HREE concentrations in Al-depleted rocks, consistent with calculated majorite fractionation trends using experimentally determined partition coefficients (Kato *et al.*, 1988; Yurimoto & Ohtani, 1992). The depletions in HREE and variations in HFSE vs REE in the Jeesiörova rocks are plotted in Fig. 7a and b. Calculated majorite fractionation trends using published partition coefficients (Yurimoto & Ohtani, 1992) do not correspond to the variations of the respective elements in the Jeesiörova rocks. Nor are the Re and Al concentrations in the Jeesiörova komatiites consistent with majorite fractionation. A previous experimental study has suggested that Re is compatible in garnet during mantle melting ($D_{Re}^{garnet/silicate\ melt} = 2.7$: Righter & Hauri, 1998). If generally true for majorite garnet, it is likely that majorite fractionation in the mantle source of the Jeesiörova komatiites would have led to significant depletion of Re. Instead, the Re concentrations in virtually all the Jeesiörova samples ($\sim$0.5–0.9 ppb: Table 2) are higher than in Al-undepleted komatiites (e.g. 0.3–0.4 ppb in Alexo komatiites: Gangopadhyay & Walker, 2003). Similarly, Al, which is a major constituent of majorite garnet, is likely to be depleted in komatiitic melts as a result of majorite fractionation during their generation. The Al_2O_3 contents of the Jeesiörova komatiites, on the other hand, are similar to those at given MgO contents of Al-undepleted rather than Al-depleted komatiites (Fig. 2a).

Collectively, the distribution patterns of moderately incompatible elements along with Re and Al concentrations in the Jeesiörova komatiites suggest that either (1) the *D* values considered for the majorite fractionation model are not appropriate for the Finnish rocks, (2) the choice of primitive mantle as a source composition is not valid, (3) majorite fractionation was not involved in the generation of these rocks and rather than being depleted in HREE, the rocks are enriched in middle REE (MREE), or (4) another petrogenetic process intervened. The first two possibilities are considered unlikely because the *D* values and/or model starting mantle parameters would have to be considerably different from those used in previous studies (e.g. Lahaye *et al.*, 1995) in order to account for the abundances of the respective elements in the Jeesiörova komatiites. The last two possibilities are discussed below.

In a different model, some of the petrological and geochemical characteristics of Barberton-type komatiites were explained in terms of hydrous melting in supra-subduction zone settings (e.g. Parman *et al.*, 1997, 2003; Grove *et al.*, 1999). For example, the negative correlation between Ti/Zr and La/Sm ratios in the chilled margins of some komatiites and komatiitic
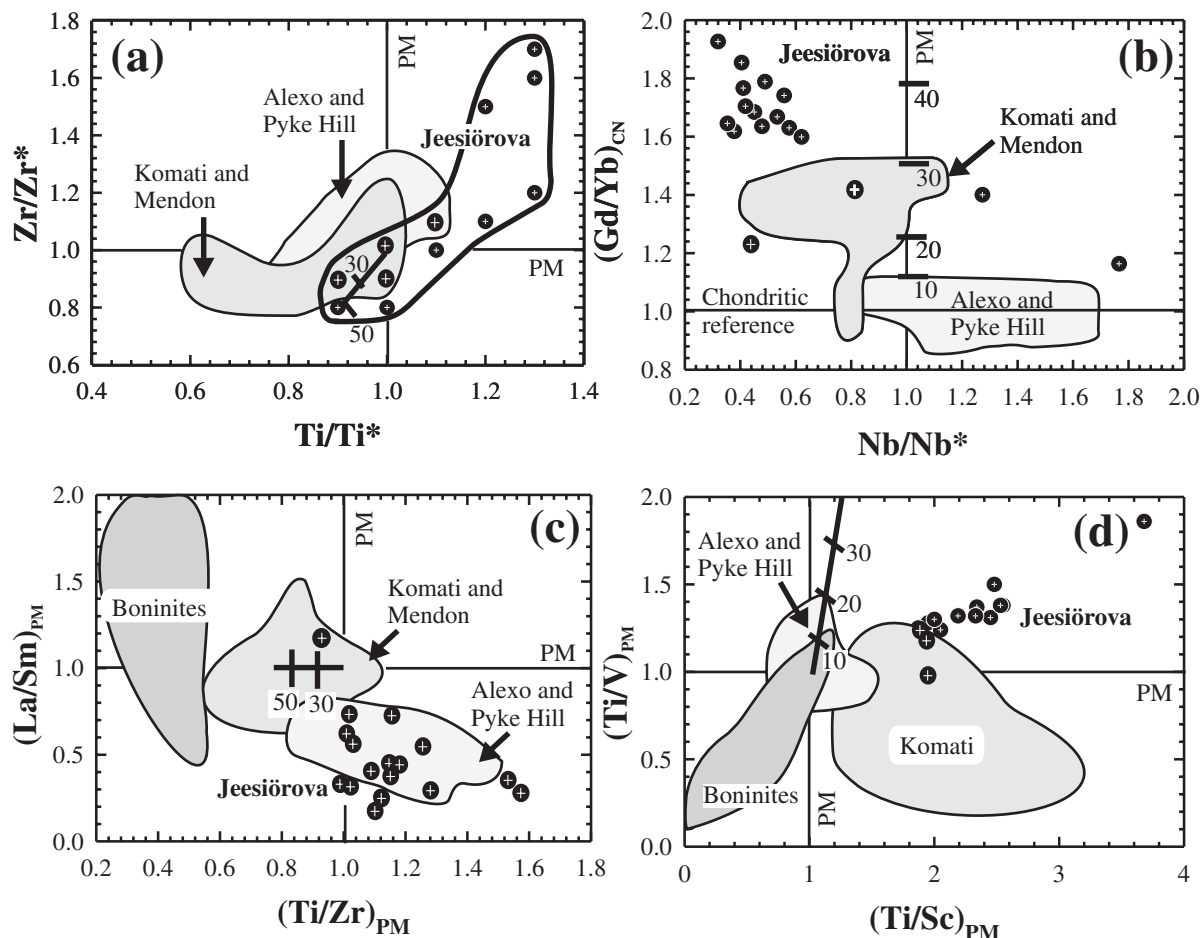
Fig. 7. Plots of HFSE anomalies (Ti, Zr and Nb) and other key trace elements in the Jeesiörova rocks compared with those for the same suites of rocks (excepting Gorgona) as in Fig. 2. The HFSE anomalies [Ti/Ti* = Ti/10$^{(\log\,Sm\,+\,3\log\,Gd)/4}$; Zr/Zr* = Zr/10$^{(\log\,Sm\,+\,\log\,Nd)/2}$; Nb/Nb* = Nb/10$^{(2\,\log\,La\,-\,\log\,Ce)}$] were calculated after McCuaig *et al.* (1994). (a) Zr/Zr* vs Ti/Ti*; (b) chondrite-normalized Gd/Yb vs Nb/Nb*; (c) PM-normalized La/Sm vs Ti/Zr; (d) PM-normalized Ti/V vs Ti/Sc. Also shown are the calculated majorite fractionation trends (continuous line with tick marks showing percentage of majorite fractionation). Data sources: $D^{majorite/liq.}$ values for each element from Yurimoto & Ohtani (1992); chondrite and PM, McDonough & Sun (1995); boninites, Hickey & Frey (1982).

basalts from Barberton resembles that observed in Phanerozoic boninites (Parman *et al.*, 2003). This feature was interpreted by Parman *et al.* (2003) as a result of mixing between a silicate melt with high La/Sm ratio and a hydrous fluid with high Ti/Zr ratio. This model is also relevant to consider here because the Jeesiörova komatiites show characteristic negative Nb anomalies (Fig. 3), similar to some Phanerozoic boninites (Hickey-Vargas, 1989) and also typically crustally contaminated tholeiites and komatiites. However, on a primitive mantle (PM)-normalized diagram of La/Sm vs Ti/Zr, the Jeesiörova rocks do not show any evidence for mixing between hydrous fluids and silicate melts compositionally similar to those that were suggested for the Barberton rocks (Fig. 7c; also see Parman *et al.*, 2003).

Additionally, as can be seen on a primitive mantle-normalized diagram of (Ti/V)$_{PM}$ vs (Ti/Sc)$_{PM}$, the Finnish rocks, unlike boninites (Hickey & Frey, 1982), are enriched rather than depleted in Ti relative to other transitional elements, such as V and Sc (Fig. 7d). Finally, the convex-up REE pattern of the Jeesiörova komatiites (Fig. 3), resulting from high concentrations of MREE relative to both LREE and HREE, is in contrast to the characteristic U-shaped REE profile of boninites (Arndt, 2003, and references therein).

In addition to their whole-rock trace element characteristics, the redox state of the Jeesiörova rocks is also unlikely to support their generation in a highly oxidized arc environment. The redox state of the Jeesiörova rocks was estimated using Fe^{3+}-number [Fe^{3+}/(Fe^{3+} + Cr +
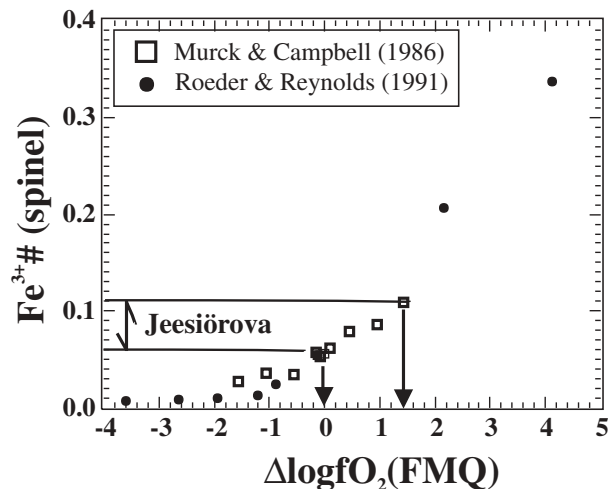
Fig. 8. Fe^{3+}-number [$Fe^{3+}/(Fe^{3+} + Cr + Al)$] of chromites in the experimental charges of Murck & Campbell (1986) and Roeder & Reynolds (1991) vs $\Delta\log fO_2$ [$\log fO_2 - \log$ (FMQ)] values for the respective experimental runs. The entire range of Fe^{3+}-numbers obtained for chromites in the Finnish rocks, as shown by the two horizontal lines, corresponds approximately to an fO_2 range of FMQ to FMQ + 1·4.

Al)] and $Fe^{3+}/\Sigma Fe$ ratios of selected chromites determined by electron microprobe and Mössbauer analysis, respectively (Table 1). The Fe^{3+}-number for the chromites in the Jeesiörova rocks, and corresponding fO_2 values, are compared with those in the 1 atm experiments of Murck & Campbell (1986) and Roeder & Reynolds (1991), which used natural komatiitic lavas as starting materials (Fig. 8). The entire range of Fe^{3+}-number of chromites in the Jeesiörova rocks corresponds approximately to a range in fO_2 from FMQ (fayalite–magnetite–quartz) to FMQ + 1·4. This range in fO_2 is consistent with that obtained for mafic–ultramafic lavas by Fisk & Bence (1980), and Barnes (1986). It is, however, recognized that conventional electron microprobe analysis of chromites does not always yield accurate estimates of fO_2, whereas the $Fe^{3+}/\Sigma Fe$ ratios of chromites determined by Mössbauer analysis are potentially more accurate for the purpose of oxygen barometry (Wood & Virgo, 1989). For this reason, the $Fe^{3+}/\Sigma Fe$ ratios of selected chromite separates from the Finnish rocks were determined by Mössbauer spectroscopy. The $Fe^{3+}/\Sigma Fe$ ratios for five chromite separates vary within a limited range of 0·16–0·28 that corresponds to fO_2 of $-1\cdot5 < \Delta FMQ < +0\cdot7$ (Parkinson & Arculus, 1999, and references therein). Thus, microprobe and Mössbauer analyses of chromites collectively yield fO_2 for the Finnish rocks of approximately $FMQ \pm 1\cdot5$. For comparison, arc-related lavas have redox states that vary from $\sim$FMQ to as high as $\sim$FMQ + 6 [as summarized by Lee *et al.* (2003)]. In contrast, estimates for the oceanic mantle as sampled by mid-ocean ridge basalt (MORB) and abyssal peridotites

are typically $\sim$FMQ to FMQ – 2. Although the entire range of fO_2 values obtained for the Jeesiörova rocks overlaps with the relatively rare, least oxidized arc rocks, it is lower than that of most arc-related rocks. Instead, the fO_2 estimates for the Jeesiörova rocks are indistinguishable from those estimated for non-arc oceanic mantle (Lee *et al.*, 2003). The range of our empirical estimates of fO_2 for the Finnish rocks is also indistinguishable from those based on the whole-rock V systematics of the Al-undepleted komatiitic basalts from Fred's Flow in the Munro Township (Canil & Fedortchouk, 2001) and, in general, with those obtained for the Archean Al-undepleted komatiites (Canil, 1999). This suggests that the redox states during the generation of both the Al-undepleted Munro rocks and the Jeesiörova komatiites were not significantly different.

The initial Os isotopic composition [$\gamma_{Os}(I) = +0\cdot1 \pm 0\cdot5$] of the mantle source of the Jeesiörova komatiites is also inconsistent with their generation in supra-subduction zone setting. Modern arc-related lavas and sub-arc mantle xenoliths commonly have variably ^{187}Os-enriched isotopic compositions that are likely to be a result of transport of radiogenic ^{187}Os via Cl-rich hydrous fluid into the mantle wedge (e.g. Brandon *et al.*, 1996, 1999; Peslier *et al.*, 2000; Lassiter & Luhr, 2001; Widom *et al.*, 2003; Saha *et al.*, 2005). The precisely chondritic initial Os isotopic composition of the Jeesiörova rocks, on the other hand, is indistinguishable from the projected Os isotopic evolution trajectory of the primitive upper mantle (PUM; Meisel *et al.*, 2001), suggesting that these rocks sampled a mantle source that had no prior history of resolvable ^{187}Os enrichment.

Are the Jeesiörova komatiites Ti enriched?

The TiO_2 contents of a significant portion of the chromites in the Jeesiörova rocks are higher than those in chromites from Al-undepleted komatiites with similar aluminum contents reported from Pyke Hill, Canada (Arndt *et al.*, 1977; Fig. 6b), Vetreny, Russia (Puchtel *et al.*, 1996) and Belingwe, Zimbabwe (Zhou & Kerrich, 1992), suggesting that the Jeesiörova parental magmas had higher Ti concentrations than those of most Al-undepleted komatiites. In most Jeesiörova whole-rock komatiites, however, mantle-normalized concentrations of Ti are similar to, or only slightly higher than, those for other moderately incompatible elements (e.g. MREE), which, in turn, appear to be enriched in comparison with less or more incompatible elements (e.g. HREE and LREE, respectively). For comparison, the entire range of Ti/Ti* in the Al-undepleted and Al-depleted komatiites is 0·6–1·1, and that in the Jeesiörova rocks is 0·9–1·3 (Fig. 9a). As noted above, the Jeesiörova komatiites have higher concentrations of Ti than in Munro- or Barberton-type rocks (Fig. 2b), yet significant
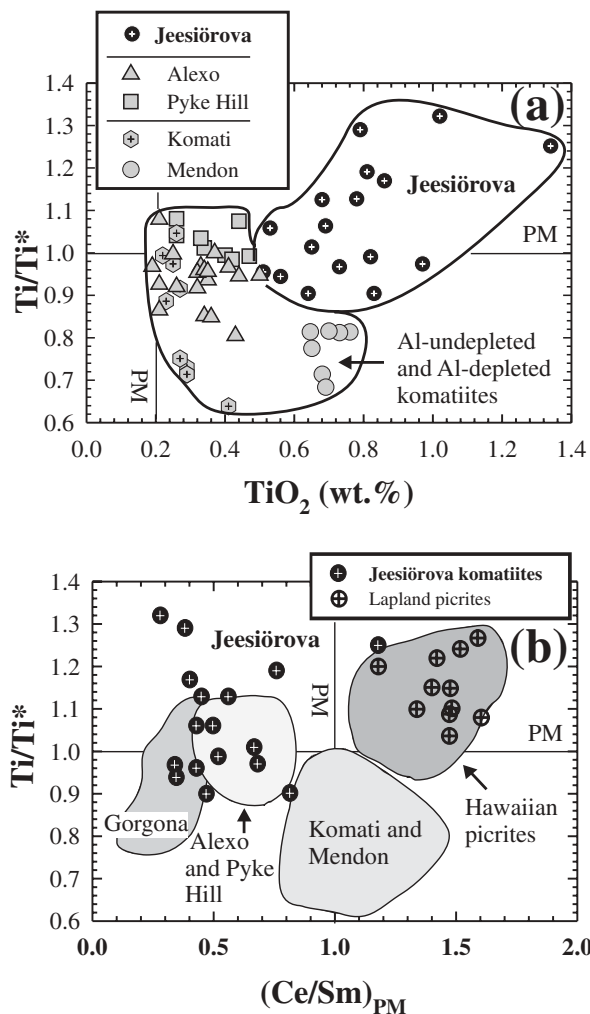
Fig. 9. (a) Whole-rock TiO_2 contents vs Ti anomalies [Ti/Ti* = $Ti/10^{(\log Sm + 3\log Gd)/4}$, calculated after McCuaig *et al.* (1994), where all the elements are normalized to PM (McDonough & Sun, 1995)] in the Jeesiörova rocks. The combined field for Al-undepleted and Al-depleted komatiites is drawn based on the data of Fig. 2, excepting data for the Alexo komatiites, which are taken from Lahaye & Arndt (1996). (b) PM-normalized Ce/Sm vs Ti/Ti* in whole-rocks of selected suites of ultramafic magmatic rocks. Data sources are as in Figs 2 and 9a. Additional data: picritic rocks from Finnish Lapland (Hanski *et al.*, 2001); Gorgona ultramafic (MgO >11 wt %) rocks (Révillon *et al.*, 2000); Hawaiian picrites (Norman & Garcia, 1999). The fields of komatiites from Gorgona, Alexo and Pyke Hill, and Komati and Mendon exclude one outlier from each of their respective datasets.

enrichments in Ti relative to similarly incompatible elements (e.g. MREE) are found only in a limited number of Jeesiörova samples (Ti/Ti* > 1·1: Fig. 9a). Elevated abundances of Ti, similar to those in the Jeesiörova rocks, are also found in komatiites from the presumed extension of the Lapland complex in the Karasjok greenstone belt, northern Norway (Barnes & Often, 1990), mafic–ultramafic lavas and sills (MgO ~14–30 wt %) from the Onega plateau in the SE Baltic Shield (Puchtel

et al., 1998), and picritic rocks from Baffin Bay, West Greenland (Clarke, 1970; Francis, 1985).

High concentrations of Ti and other moderately incompatible elements as a feature of the mantle source

Based on the major and trace element characteristics of the Ti-rich komatiites from the Karasjok greenstone belt, northern Norway, Barnes & Often (1990) concluded that the Ti-rich nature of the Norwegian rocks is unlikely to be a result of (1) post-magmatic alteration, (2) crustal contamination or (3) lower degrees of melting. These possibilities for the Jeesiörova rocks are considered briefly below.

First, it is possible that elevated concentrations of some HFSE, such as Ti and Zr, could result from the loss of other elements or addition of HFSE during some stage of alteration. However, Ti and Zr are among the least mobile elements during alteration of komatiites (e.g. Arndt, 1994), and there are strong negative correlations on plots of MgO vs TiO_2 (see Hanski *et al.*, 2001) and Zr in the Jeesiörova rocks. This strongly suggests that Ti abundances were not significantly affected during secondary alteration. Second, the Jeesiörova parental magmas are unlikely to have suffered a large degree of contamination by old continental crustal materials. The LREE-depleted nature and ^{143}Nd-enriched initial isotopic composition of the Jeesiörova rocks (ε_{Nd} ~+4: Hanski *et al.*, 2001) is consistent with their derivation from a source similar to the contemporaneous depleted upper mantle (DePaolo, 1981), suggesting that these komatiites were not significantly contaminated by typical continental crustal materials. Importantly, Ti contents in most crustal rocks are significantly lower than in the Jeesiörova komatiites, so the high concentrations of Ti are not a result of crustal contamination. Third, the high relative concentrations of Ti and moderately incompatible elements in the Jeesiörova komatiites are probably not due solely to lower degrees of partial melting of the mantle source than for the Munro- or Barberton-type rocks. This is because the incompatibility of Ti during mantle melting is intermediate between that of Eu and Gd (MREE), and significantly lower than that of the LREE (Sun & McDonough, 1989). Accordingly, for the case of modal batch melting, the rate of increase in LREE/MREE (e.g. Ce/Sm) in the partial melt as a function of degree of melting is likely to be higher than that for Ti/MREE (e.g. Ti/Ti*; see Rollinson, 1998). For comparison, high Ti contents in picrites from both Hawaii and Finnish Lapland, which are presumably products of lower degrees of partial melting than Munro-type komatiites, are accompanied by corresponding increases in Ce/Sm ratios (Norman & Garcia, 1999; Hanski *et al.*, 2001; Fig. 9b). No such correlation is

observed for the Jeesiörova komatiites, and, instead, the komatiite samples with the highest Ti concentrations (and also highest Ti/Ti*) are typically the most LREE depleted (Fig. 9b). This combination of the most elevated Ti concentrations and lowest LREE/MREE in some Jeesiörova samples is not found among the Barberton- or Munro-type rocks. Consequently, it is difficult to envision known melting scenarios in which the high concentrations of Ti and other moderately incompatible elements in Jeesiörova rocks could have been produced from a mantle source, similar in degree of LREE depletion to that of the Munro komatiites, solely as a result of lower degrees of melting. It is more likely that, regardless of the absolute degree of melting of the Jeesiörova mantle source, the higher Ti concentrations (Fig. 2b) are due to process(es) other than differential degrees of melting relative to the Munro komatiites. For example, it is possible that either the mantle source for the Jeesiörova komatiites had higher relative concentrations of Ti and other moderately incompatible elements than the Abitibi mantle source and/or the primary Jeesiörova magmas underwent subsequent enrichments in these elements *en route* to the surface. These two possibilities are discussed below.

Consideration of alternative petrogenetic processes

Assimilation of phases rich in moderately incompatible elements

First, we consider the possibility that the overall convexup REE patterns of the Jeesiörova komatiites (Fig. 3) were the result of selective enrichment of the primary magmas in MREE and other moderately incompatible elements (e.g. Ti, Zr) relative to both LREE and HREE. For example, the high concentrations of Ti, Zr and MREE in the Jeesiörova komatiites could, potentially, have resulted from selective assimilation of phases rich in moderately incompatible elements during ascent of the magma through the lithosphere. The high Ti and Zr abundances in the Jeesiörova komatiites are coupled with slightly suprachondritic Zr/Hf ratios (typically 42–46 relative to the chondritic value of 36: McDonough & Sun, 1995). Moreover, the rocks show a broad positive correlation between Ti/Ti* and Zr/Zr*, and samples that have the highest values of Ti/Ti* also typically have the largest positive Zr anomalies (Zr/Zr* up to 1·7: Fig. 7a). Some Ti-rich minerals (e.g. rutile, armalcolite, loveringite) produced by metasomatism within the sub-continental lithospheric mantle (SCLM), as sampled by peridotite xenoliths, commonly show high abundances of HFSE and also suprachondritic Zr/Hf ratios (up to 58: Kalfoun *et al.*, 2002). Despite very low modal abundances, these minerals can account for >50% of HFSE budgets in some whole-rock peridotite xenoliths (Kalfoun *et al.*, 2002). Ti-rich metasomatic mineral assemblages

(rutile, ilmenite, armalcolite) have also been documented in harzburgitic oceanic mantle xenoliths from the Kerguelen Islands that are likely to have crystallized at temperatures of ∼1200°C, consistent with the relatively low melting temperatures for these minerals (Grégoire *et al.*, 2000).

Selective assimilation of phases rich in moderately incompatible elements by low-Ti primary melts in the generation of the Jeesiörova parental magmas is consistent with some experimental studies. For example, the dissolution rate experiments of Wagner & Grove (1997) suggest that Ti-rich oxide minerals, such as ilmenite, melt out ∼3 times faster than clinopyroxene in a typical mineral assemblage in the lunar mantle. Wagner & Grove inferred that some high-Ti lunar magmas were produced from low-Ti primitive magmas via assimilation of ilmenite-rich assemblages at shallow levels. Similarly, high-pressure and high-temperature melting experiments on terrestrial picritic basalt compositions suggest that near-solidus melts produced from armalcolite (± ilmenite)-bearing peridotites have very high TiO_2 contents (≥20 wt %: Xirouchakis *et al.*, 2001) consistent with preferential non-modal melting of Ti-rich phases.

It might also be expected that significant interaction of the parental komatiite melts with the SCLM would lead to a reduction in the initial $^{187}Os/^{188}Os$ of the magmas. This is because it is commonly observed that the SCLM has depleted $^{187}Os/^{188}Os$ relative to the contemporaneous convecting upper mantle as a result of prior Re depletion (Walker *et al.*, 1989). For example, combined Os–Nd isotope characteristics have been used to support up to ∼50% contribution of lithospheric components in the generation of ∼190 Ma Karoo picrites (Ellam *et al.*, 1992). This interpretation was based on the correspondence of the Karoo picrites in an Os–Nd isotope diagram to a calculated mixing array plotting between assumed plume (both high γ_{Os} and ϵ_{Nd}) and SCLM (both low γ_{Os} and ϵ_{Nd}) end-members. Another possible manifestation of such a process may be found in the ∼2·7 Ga Al-depleted ultramafic rocks from Boston Creek (Abitibi greenstone belt), which have strongly depleted initial Os isotopic compositions [$\gamma_{Os}(I) = -3\cdot8 \pm 0\cdot5$: Walker & Stone, 2001]. The chondritic Os isotopes, combined with the depleted mantle-like Nd isotopic composition of the Jeesiörova rocks, on the other hand, argues against bulk mixing of large proportions of these components, as a mixing array rather than uniform Nd–Os isotopic compositions for these rocks would be expected.

The uniform chondritic initial Os isotopic composition of the Jeesiörova rocks may suggest that either (1) assimilation of metasomatized lithospheric minerals was not involved, (2) insufficient time between the metasomatic event(s) that produced the lithospheric minerals and their melting precluded significant enrichment or depletion in ^{187}Os relative to that of the contemporaneous convecting

upper mantle, or (3) Os concentrations in the putative metasomatized mineral assemblages were significantly lower than in the primitive Jeesiörova magmas. Consistent with the last possibility, the phases rich in Ti (picroilmenite) in alkaline ultramafic magmas from Norseman–Wiluna belt, Western Australia, have very low concentrations of Os (0·02–0·03 ppb: Graham *et al.*, 2002) that are two orders of magnitude lower than those in whole-rock Jeesiörova komatiites (Table 2). In the absence of Os concentrations and isotopic compositions for metasomatized mineral assemblages in xenoliths from the SCLM that the Jeesiörova magmas must have traversed, the likelihood of the last two possibilities [(2) and (3)], cannot yet be evaluated.

Enrichment of the Jeesiörova mantle source by basaltic melts

The high concentrations of moderately incompatible elements in the Jeesiörova rocks, combined with their radiogenic initial Nd isotopic composition (ε_{Nd} ∼+4: Hanski *et al.*, 2001) and LREE-depleted nature, may, alternatively, have resulted from enrichment of the mantle source by basaltic melts or incorporation of young recycled mafic oceanic crust, similar to depleted normal mid-oceanic ridge basalts (N-MORB), into the mantle source. This possibility is consistent with the higher average abundance of most incompatible elements in the Jeesiörova komatiites relative to typical Al-undepleted and Al-depleted komatiites. The Os concentrations of MORB (e.g. 0·23–31·8 ppt: Schiano *et al.*, 1997) are 2–3 orders of magnitude lower than in likely depleted peridotitic mantle sources for komatiites (e.g. empirical estimates of 3·9 ppb Os for the source of Abitibi komatiites: Puchtel *et al.*, 2004), so the chondritic initial Os isotopic composition of the mixed source for the Jeesiörova komatiites could essentially represent that of the peridotite component. The long-term [143]Nd-enriched initial isotopic composition of the Jeesiörova rocks, on the other hand, may reflect contributions from both LREE-depleted N-MORB and peridotite source components. Furthermore, enrichment of the peridotite source by mafic melts may lead to an increase in Re concentrations, so this process could account for higher relative Re concentrations in these komatiites. The high Re/Os ratios of the mantle source, over time, would potentially lead to growth of suprachondritic $^{187}Os/^{188}Os$. Therefore, the chondritic initial $^{187}Os/^{188}Os$ of the Jeesiörova rocks suggests that mafic enrichment of the source could not have occurred more than ∼200 Myr prior to komatiite production (see Walker *et al.*, 1991).

Neither of the two petrogenetic processes discussed above, however, is consistent with all aspects of the Jeesiörova komatiites. For example, the presence of uniform negative Nb anomalies in the Jeesiörova rocks

(Figs 3 and 7b) cannot be readily reconciled with models of trace element enrichment via addition of basaltic melt or recycled oceanic crust to their mantle source. Present-day N-MORB does not have negative Nb anomalies, and, therefore, recycling of oceanic crust would require that the LREE-depleted primary Jeesiörova asthenospheric melts possessed negative Nb anomalies to begin with: a possibility for which there are no known analogs (Hofmann, 1988; Salters & Stracke, 2004, and references therein). Similarly, neither assimilation of hypothetical lithospheric mantle phases nor prior basaltic melt enrichment of the source can cause the apparent HREE depletion of the Jeesiörova komatiites, which is commonly explained in terms of fractionation of majorite garnet during the generation of the mantle-derived magmas (Hofmann, 1988; Gurenko & Chaussidon, 1995; Arndt *et al.* 1997). Furthermore, if either of the petrogenetic processes suggested above occurred in combination with majorite fractionation at some stage in the generation of the Jeesiörova rocks, it remains unclear as to why their HREE depletion is neither accompanied by correspondingly low Al_2O_3 contents (Fig. 2a) nor correlated with other geochemical parameters suggestive of majorite fractionation (Fig. 7a–d), similar to those commonly observed in Barberton-type komatiites.

CONCLUSIONS

The Jeesiörova komatiites have subchondritic Al_2O_3/TiO_2 ratios and HREE depletion ($Gd/Yb_{CN} >1$), similar to those typically observed in Al-depleted komatiites. We have demonstrated that the subchondritic Al_2O_3/TiO_2 in the Jeesiörova rocks is not a result of depletion in Al, but rather is due to high concentrations of Ti at a given MgO content relative to both Al-undepleted and Al-depleted komatiites. The Jeesiörova rocks also have overall high concentrations of moderately incompatible elements relative to these two types of komatiite and, thus, represent a chemically distinct type of komatiite. The whole-rock major and trace element characteristics (e.g. absence of depletion in Al corresponding to HREE depletion), and redox state (∼FMQ) estimated from the chemical composition of chromite, are not consistent with either of the petrogenetic models suggested for the Al-depleted rocks, majorite fractionation in the deep mantle or hydrous melting in a supra-subduction zone setting. The high relative concentrations of Ti and similarly incompatible elements in these rocks may suggest either (1) assimilation of metasomatized mineral assemblages rich in moderately incompatible elements present in the lithospheric mantle or (2) contamination of the source of the primary asthenospheric melts by young LREE-depleted oceanic crust. The characteristic negative Nb anomalies in the Jeesiörova rocks, however,

are not consistent with any of these models. Nevertheless, the combined Os–Nd isotopic characteristics suggest that their mantle source, regardless of the mechanism responsible for the distinctively high concentrations of moderately incompatible elements, is indistinguishable from the contemporaneous convecting upper mantle.

ACKNOWLEDGEMENTS

SUPPLEMENTARY DATA

Supplementary data on this paper are available at *Journal of Petrology* online.

REFERENCES

Arndt, N. (1986). Differentiation of komatiite flows. *Journal of Petrology* **27**, 279–301.

Arndt, N. T. (1994). Archean komatiites. In: Kondie, K. C. (ed.) *Archean Crustal Evolution*. Amsterdam: Elsevier, pp. 11–44.

Arndt, N. T. (2003). Komatiites, kimberlites, and boninites. *Journal of Geophysical Research* **108**, 1–11.

Arndt, N. T., Naldrett, A. J. & Pyke, D. R. (1977). Komatiitic and iron-rich tholeiitic lavas from Munro Township, northeast Ontario. *Journal of Petrology* **18**, 319–369.

Arndt, N. T., Kerr, A. C. & Tarney, J. (1997). Dynamic melting in plume heads: the formation of Gorgona komatiites and basalts. *Earth and Planetary Science Letters* **146**, 289–301.

Barnes, Sarah-Jane & Often, M. (1990). Ti-rich komatiites from Northern Norway. *Contributions to Mineralogy and Petrology* **105**, 42–54.

Barnes, Stephen J. (1986). The distribution of chromium among orthopyroxene, spinel and silicate liquid at atmospheric pressure. *Geochimica et Cosmochimica Acta* **50**(9), 1889–1909.

Barnes, Stephen J. & Roeder, P. (2001). The range of spinel compositions in terrestrial mafic and ultramafic rocks. *Journal of Petrology* **42**(12), 2279–2302.

Brandon, A. D., Creaser, R. A., Shirey, S. B. & Carlson, R. W. (1996). Osmium recycling in subduction zones. *Science* **272**, 861–864.

Brandon, A. D., Becker, H., Carlson, R. W. & Shirey, S. B. (1999). Isotopic constraints on time scales and mechanisms of slab material transport in the mantle wedge: evidence from the Simcoe mantle xenoliths, Washington, USA. *Chemical Geology* **160**, 387–408.

Brandon, A. D., Snow, J., Walker, R. J., Morgan, J. W. & Mock, T. D. (2000). $^{190}Pt–^{186}Re$ and $^{187}Re–^{187}Os$ systematics of abyssal peridotites. *Earth and Planetary Science Letters* **177**, 319–335.

Canil, D. (1999). Vanadium partitioning and the oxidation state of Archean komatiite magmas. *Nature* **389**, 842–845.

Canil, D. & Fedortchouk, Y. (2001). Olivine–liquid partitioning of vanadium and other trace elements, with applications to modern and ancient picrites. *Canadian Mineralogist* **39**, 319–330.

Clarke, D. B. (1970). Tertiary basalts of Baffin Bay: possible primary magma from the mantle. *Contributions to Mineralogy and Petrology* **25**, 203–224.

Cohen, A. S. & Waters, F. J. (1996). Separation of osmium from geological materials by solvent extraction for analysis by TIMS. *Analytica Chimica Acta* **332**, 269–275.

Creaser, R. A., Papanastassiou, D. A. & Wasserburg, G. J. (1991). Negative thermal ion mass spectrometry of osmium, rhenium and iridium. *Geochimica et Cosmochimica Acta* **55**, 397–401.

DePaolo, D. J. (1981). Neodymium isotopes in the Colorado Front Range and implications for crust formation and mantle evolution in the Proterozoic. *Nature* **291**, 193–197.

Echeverria, L. M. (1980). Tertiary or Mesozoic komatiites from Gorgona Island, Colombia: field relations and geochemistry. *Contributions to Mineralogy and Petrology* **73**, 253–266.

Eggins, S. M. (1993). Origin and differentiation of picritic arc magmas, Ambae (Aoba), Vanuatu. *Contributions to Mineralogy and Petrology* **114**, 79–100.

Ellam, R. M., Carlson, R. W. & Shirey, S. B. (1992). Evidence from Re–Os isotopes for plume–lithosphere mixing in Karoo flood basalt genesis. *Nature* **359**, 718–721.

Fan, J. & Kerrich, R. (1997). Geochemical characteristics of aluminum depleted and undepleted komatiites and HREE-enriched low-Ti tholeiites, western Abitibi greenstone belt: a heterogeneous mantle plume–convergent margin environment. *Geochimica et Cosmochimica Acta* **61**(22), 4723–4744.

Fisk, M. R. & Bence, A. E. (1980). Experimental crystallization of chrome spinel in FAMOUS basalt 527-1-1. *Earth and Planetary Science Letters* **48**(1), 111–123.

Francis, D. (1985). The Baffin Bay lavas and the value of picrites as analogues of primary magmas. *Contributions to Mineralogy and Petrology* **89**, 144–154.

Gangopadhyay, A. (2004). A petrologic, geochemical and Os isotopic study of selected Precambrian komatiites. Ph.D. dissertation, University of Maryland, College Park. http://hdl.handle.net/1903/2011.

Gangopadhyay, A. & Walker, R. J. (2003). Re–Os systematics of the *ca*. 2·7-Ga komatiites from Alexo, Ontario, Canada. *Chemical Geology* **196**, 147–162.

Gangopadhyay, A., Sproule, R. A., Walker, R. J. & Lesher, C. M. (2005). Re–Os systematics of komatiites and komatiitic basalts at Dundonald Beach, Ontario, Canada: evidence for a complex alteration history and implications of a late-Archean chondritic mantle source. *Geochimica et Cosmochimica Acta* **69**, 5087–5098.

Graham, S., Lambert, D. D., Shee, S. R. & Pearson, N. J. (2002). Juvenile lithospheric mantle enrichment and the formation of alkaline ultramafic magma sources: Re–Os, Lu–Hf and Sm–Nd isotopic systematics of the Norseman melnoites, Western Australia. *Chemical Geology* **186**, 215–233.

Grégoire, M., Lorand, J. P., O'Reilly, S. Y. & Cottin, J. Y. (2000). Armalcolite-bearing, Ti-rich metasomatic assemblages in harzburgitic xenoliths from the Kerguelen Islands: implications for the oceanic mantle budget of high-field strength elements. *Geochimica et Cosmochimica Acta* **64**, 673–694.

Grove, T. L., Parman, S. W. & Dann, J. C. (1999). Conditions of magma generation for Archean komatiites from the Barberton Mountainland, South Africa. In: Fei, Y., Bertka, C. & Mysen, B. O. (eds) *Mantle Petrology: Field Observations and High Pressure Experimentation: a Tribute to Francis R. (Joe) Boyd. Geochemical Society Special Publication* **6**, 155–167.

Gurenko, A. A. & Chaussidon, M. (1995). Enriched and depleted primitive melts included in olivine from Icelandic tholeiites: origin by continuous melting of a single mantle column. *Geochimica et Cosmochimica Acta* **59**, 2905–2917.

Hanski, E., Huhma, H., Rastas, P. & Kamenetsky, V. S. (2001). The Palaeoproterozoic komatiite–picrite association of Finnish Lapland. *Journal of Petrology* **42**(5), 855–876.

Herzberg, C. (1995). Generation of plume magmas through time: an experimental perspective. *Chemical Geology* **126**, 1–16.

Hickey, R. L. & Frey, F. A. (1982). Geochemical characteristics of boninite series volcanics: implications for their source. *Geochimica et Cosmochimica Acta* **46**, 2099–2115.

Hickey-Vargas, R. (1989). Boninites and tholeiites from DSDP Site 458, Mariana forearc. In: Crawford, A. J. (ed.) *Boninites*. New York: Chapman and Hall, pp. 257–356.

Hofmann, A. W. (1988). Chemical differentiation of the Earth: the relationship between mantle, continental crust, and oceanic crust. *Earth and Planetary Science Letters* **90**, 297–314.

Kalfoun, F., Ionov, D. & Merlet, C. (2002). HFSE residence and Nb/Ta ratios in metasomatised, rutile-bearing mantle peridotites. *Earth and Planetary Science Letters* **199**, 49–65.

Kato, T., Ringwood, A. E. & Irifune, T. (1988). Experimental determination of element partitioning between silicate perovskites, garnets and liquids: constraints on early differentiation of the mantle. *Earth and Planetary Science Letters* **89**, 123–145.

Lahaye, Y. & Arndt, N. (1996). Alteration of a komatiite flow from Alexo, Ontario, Canada. *Journal of Petrology* **37**(6), 1261–1284.

Lahaye, Y., Arndt, N., Byerly, G., Chauvel, C., Fourcade, S. & Gruau, G. (1995). The influence of alteration on the trace-element and Nd isotopic compositions of komatiites. *Chemical Geology* **126**, 43–64.

Lassiter, J. C. & Luhr, J. F. (2001). Osmium abundance and isotope variations in mafic Mexican volcanic rocks: evidence for crustal contamination and constraints on the geochemical behavior of osmium during partial melting and fractional crystallization. *Geochemistry, Geophysics, Geosystems* **2**, 2000GC000116.

Lee, C.-T. A., Brandon, A. D. & Norman, M. (2003). Vanadium in peridotites as a proxy for paleo-fO_2 during partial melting: prospects, limitations and implications. *Geochimica et Cosmochimica Acta* **67**(16), 3045–3064.

Lehtonen, M., Airo, M.-L., Eilu, P., Hanski, E., Kortelainen, V., Lanne, E., Manninen, T., Rastas, P., Räsänen, J. & Virransalo, P. (1998). Kittilän alueen geologia. Lapin vulkaniittiprojektin raportti. Summary: the stratigraphy, petrology and geochemistry of the Kittilä greenstone area, northern Finland. A Report of the Lapland Volcanite Project. *Geological Survey of Finland Report of Investigation* **140**, 144 pp.

Luck, J.-M. & Allègre, C. J. (1984). $^{187}Re/^{187}Os$ investigation in sulfide from Cape Smith komatiite. *Earth and Planetary Science Letters* **68**, 205–208.

McCuaig, T. C., Kerrich, R. & Xie, Q. (1994). Phosphorus and high field strength element anomalies in Archean high-magnesian magmas as possible indicators of source mineralogy and depth. *Earth and Planetary Science Letters* **124**, 221–239.

McDonough, W. F. & Sun, S.-s. (1995). The composition of the Earth. *Chemical Geology* **120**, 223–253.

Meisel, T., Walker, R. J., Irving, A. & Lorand, J. P. (2001). Osmium isotopic compositions of mantle xenoliths: a global perspective. *Geochimica et Cosmochimica Acta* **65**(8), 2331–2344.

Morgan, J. W. & Walker, R. J. (1989). Isotopic determinations of rhenium and osmium in meteorites by using fusion, distillation and ion exchange separations. *Analytica Chimica Acta* **222**, 291–300.

Morgan, J. W., Horan, M. F., Walker, R. J. & Grossman, J. N. (1995). Rhenium–osmium concentration and isotope systematics in group IIAB iron meteorites. *Geochimica et Cosmochimica Acta* **59**, 2331–2344.

Murck, B. W. & Campbell, I. H. (1986). The effects of temperature, oxygen fugacity and melt composition on the behavior of chromium in basic and ultrabasic melts. *Geochimica et Cosmochimica Acta* **50**, 1871–1887.

Nesbitt, R. W. & Sun, S.-S. (1976). Geochemistry of Archean spinifex-textured peridotites and magnesian and low-magnesian tholeiites. *Earth and Planetary Science Letters* **31**, 433–453.

Nesbitt, R. W., Sun, S.-S. & Purvis, A. C. (1979). Komatiites: geochemistry and genesis. *Canadian Mineralogist* **17**, 165–186.

Norman, M. D. & Garcia, M. O. (1999). Primitive magmas and source characteristics of the Hawaiian plume: petrology and geochemistry of shield picrites. *Earth and Planetary Science Letters* **168**, 27–44.

Parkinson, I. J. & Arculus, R. J. (1999). The redox state of subduction zones: insights from arc-peridotites. *Chemical Geology* **160**, 409–423.

Parman, S. W., Dann, J. C., Grove, T. L. & de Wit, M. J. (1997). Emplacement conditions of komatiite magmas from the 3·49 Ga Komati Formation, Barberton Greenstone Belt, South Africa. *Earth and Planetary Science Letters* **150**, 303–323.

Parman, S. W., Shimizu, N., Grove, T. L. & Dann, J. C. (2003). Constraints on the pre-metamorphic trace element composition of Barberton komatiites from ion probe analyses of preserved clinopyroxene. *Contributions to Mineralogy and Petrology* **144**, 383–396.

Peslier, A. H., Reisberg, L., Ludden, J. & Francis, D. (2000). Re–Os constraints on harzburgite and lherzolite formation in the lithospheric mantle: a study of northern Canadian Cordillera xenoliths. *Geochimica et Cosmochimica Acta* **64**, 3061–3071.

Puchtel, I. S., Hofmann, A. W., Mezger, K., Shchipansky, A. A., Kulikov, V. S. & Kulikova, V. V. (1996). Petrology of a 2·41 Ga remarkably fresh komatiitic basalt lava lake in Lion Hills, central Vetreny Belt, Baltic Shield. *Contributions to Mineralogy and Petrology* **124**, 273–290.

Puchtel, I. S., Arndt, N. T., Hoffman, A. W., Hasse, K. M., Kröner, A., Kulikov, V. S., Kulikova, V. V., Garbe-Schönberg, C.-D. & Nemchin, A. A. (1998). Petrology of mafic lavas within the Onega plateau, central Karelia: evidence for 2·0 Ga plume-related continental crustal growth in the Baltic Shield. *Contributions to Mineralogy and Petrology* **130**, 134–153.

Puchtel, I. S., Humayun, M., Campbell, A. J., Sproule, R. A. & Lesher, C. M. (2004). Platinum group element geochemistry of komatiites from the Alexo and Pyke Hill areas, Ontario, Canada. *Geochimica et Cosmochimica Acta* **68**, 1361–1383.

Pyke, D. R., Naldrett, A. J. & Eckstrand, O. R. (1973). Archean ultramafic flows in Munro Township, Ontario. *Geological Society of America Bulletin* **84**, 955–978.

Révillon, S., Arndt, N. T., Chauvel, C. & Hallot, E. (2000). Geochemical study of ultramafic volcanic and plutonic rocks from Gorgona Island, Colombia: the plumbing system of an oceanic plateau. *Journal of Petrology* **41**(7), 1127–1153.

Righter, K. & Hauri, E. (1998). Compatibility of rhenium in garnet during mantle melting and magma genesis. *Science* **280**, 1737–1741.

Roeder, P. L. & Reynolds, I. (1991). Crystallization of chromite and chromium solubility in basaltic melt. *Journal of Petrology* **32**, 909–934.

Rollinson, H. R. (1998). *Using Geochemical Data: Evaluation, Presentation, Interpretation.* Harlow: Longman.

Saha, A., Basu, A. R., Jacobsen, S. B., Poreda, R. J., Yin, Q.-Z. & Yogodzinski, G. M. (2005). Slab devolatilization and Os and Pb mobility in the mantle wedge of the Kamchatka Arc. *Earth and Planetary Science Letters* **236**, 182–194.

Salters, V. J. M. & Stracke, A. (2004). Composition of the depleted mantle. *Geochemistry, Geophysics, Geosystems* **5**(5), doi:10.1029/2003GC000597.

Saverikko, M. (1985). The pyroclastic komatiite complex at Sattasvaara in northern Finland. *Bulletin of the Geological Society of Finland* **57**, 55–87.

Schiano, P., Birck, J.-L. & Allègre, C. J. (1997). Osmium–strontium–neodymium–lead isotopic covariations in mid-ocean ridge basalt glasses and the heterogeneity of the upper mantle. *Earth and Planetary Science Letters* **150**, 363–379.

Shirey, S. B. & Walker, R. J. (1995). Carius tube digestion for low-blank rhenium–osmium analyses. *Analytical Chemistry* **34**, 2136–2141.

Shirey, S. B. & Walker, R. J. (1998). The Re–Os isotope system in cosmochemistry and high-temperature geochemistry. *Annual Review of Earth and Planetary Sciences* **26**, 423–500.

Smoliar, M. I., Walker, R. J. & Morgan, J. W. (1996). Re–Os ages of group IIA, IIIA, IVA and IVB iron meteorites. *Science* **271**, 1099–1102.

Snow, J. E. & Reisberg, L. (1995). Os isotopic systematics of the MORB mantle: results from altered abyssal peridotites. *Earth and Planetary Science Letters* **133**, 411–421.

Sproule, R., Lesher, C. M., Ayer, J. A., Thurston, P. C. & Herzberg, C. T. (2002). Spatial and temporal variations in the geochemistry of komatiites and komatiitic basalts in the Abitibi greenstone belt. *Precambrian Research* **115**, 153–186.

Sun, S.-S. & McDonough, W. F. (1989). Chemical and isotopic systematics of oceanic basalts: implications for mantle composition and processes. In: Saunders, A. D. & Norry, M. J. (eds) *Magmatism in the Ocean Basins. Geological Society, London, Special Publications* **42**, 313–345.

Völkening, J., Walczyk, T. & Heumann, K. (1991). Osmium isotope ratio determinations by negative thermal ionization mass spectrometry. *International Journal of Mass Spectrometry and Ion Processes* **105**, 147–159.

Wagner, T. P. & Grove, T. L. (1997). Experimental constraints on the origin of lunar high-Ti ultramafic glasses. *Geochimica et Cosmochimica Acta* **61**, 1315–1327.

Walker, R. J. & Stone, W. R. (2001). Os isotopic constraints on the origin of the 2·7 Ga Boston Creek flow, Ontario, Canada. *Chemical Geology* **175**, 567–579.

Walker, R. J., Carlson, R. W., Shirey, S. B. & Boyd, F. R. (1989). Os, Sr, Nd, and Pb isotope systematics of southern African peridotite xenoliths: implications for the chemical evolution of subcontinental mantle. *Geochimica et Cosmochimica Acta* **53**, 1583–1595.

Walker, R. J., Echeverría, L. M., Shirey, S. B. & Horan, M. F. (1991). Re–Os isotopic constraints on the origin of volcanic rocks, Gorgona Island, Colombia: Os isotopic evidence for ancient heterogeneities in the mantle. *Contributions to Mineralogy and Petrology* **107**, 150–162.

Walker, R. J., Morgan, J. W., Horan, M. F., Czamanske, G. K., Krogstad, E. J., Fedorenko, V. & Kunilov, V. E. (1994). Re–Os isotopic evidence for an enriched-mantle source for the Noril'sk-type ore-bearing intrusion, Siberia. *Geochimica et Cosmochimica Acta* **58**, 4179–4197.

Walker, R. J., Hanski, E., Vuollo, J. & Liipo, J. (1996). The Os isotopic composition of Proterozoic upper mantle: evidence for chondritic upper mantle from the Outokumpu ophiolite, Finland. *Earth and Planetary Science Letters* **141**, 161–173.

Walker, R. J., Morgan, J. W., Hanski, E. J. & Smolkin, V. F. (1997). Re–Os systematics of Early Proterozoic ferropicrites, Pechenga Complex, northwestern Russia: evidence for ancient ^{187}Os-enriched plumes. *Geochimica et Cosmochimica Acta* **61**, 3145–3160.

Walker, R. J., Prichard, H. M., Ishiwatari, A. & Pimentel, M. (2002). The Os isotopic composition of the convecting upper mantle deduced from ophiolite chromites. *Geochimica et Cosmochimica Acta* **66**, 329–345.

Widom, E., Kepezhinskas, P. & Defant, M. (2003). The nature of metasomatism in the sub-arc mantle wedge: evidence from Re–Os isotopes in Kamchatka peridotite xenoliths. *Chemical Geology* **196**, 283–306.

Wood, B. J. & Virgo, D. (1989). Upper mantle oxidation state: ferric iron contents of lherzolite spinels by ^{57}Fe Mössbauer spectroscopy and resultant oxygen fugacities. *Geochimica et Cosmochimica Acta* **53**, 1277–1291.

Xie, Q. & Kerrich, R. (1994). Silicate-perovskite and majorite signature in komatiites from the Archean Abitibi greenstone belt: implications for early mantle differentiation and stratification. *Journal of Geophysical Research* **99**, 15799–15812.

Xirouchakis, D., Hirschmann, M. M. & Simpson, J. A. (2001). The effect of titanium on the silica content and on mineral–liquid partitioning of mantle-equilibrated melts. *Geochimica et Cosmochimica Acta* **65**, 2201–2217.

Yurimoto, H. & Ohtani, E. (1992). Element partitioning between majorite and liquid: a secondary ion mass spectrometric study. *Geophysical Research Letters* **19**, 17–20.

Zhou, M. & Kerrich, R. (1992). Morphology and composition of chromite in komatiites from the Belingwe greenstone belt, Zimbabwe. *Canadian Mineralogist* **30**, 303–317.